Metallation pathway of a plant metallothionein: Cicer arietinum MT2

Salim, Alma ; Chesnov, Serge ; Freisinger, Eva

Abstract: The plant metallothionein 2 protein from Cicer arietinum (cicMT2) is a typical member of the plant MT subfamily p2 that is characterized by an N- and C-terminal cysteine- (Cys-)rich, metal binding sequence connected by a long cysteine-free linker region. cicMT2 coordinates up to five ZnII or CdII ions by its 14 cysteine thiolate groups forming a single metal-thiolate cluster. While MTs from other phyla are considerably well-studied, many details about plant MTs are missing. In this study the metallation pathway of cicMT2 is investigated using mass spectrometry. To evaluate the influence of the linker region as well as the interplay of the two Cys-rich stretches, the full-length cicMT2 protein as well as the individual Cys-rich domains with and without the linker region were analysed. Up to three CdII ions can be coordinated by the eight Cys residues of the N-terminal part and up to two CdII ions by the six Cys residues of the C-terminal sequence. However, no preferential binding to either of the two sequences is observed, which is in-line with the closely similar apparent binding constants of the individual domains obtained from competition reactions with the chelator 1,2-bis(2-amino-5-fluorophenoxy)ethane-N,N,N ,N -tetraacetic acid. The combination of limited proteolytic digestion, mass spectrometry, dynamic light scattering, size-exclusion chromatography, and 19F NMR spectroscopy enables us to draw conclusions about the overall protein-fold and the cluster formation process.

DOI: https://doi.org/10.1016/j.jinorgbio.2020.111157

Journal of Inorganic Biochemistry 210 (2020) 111157

Contents lists available at ScienceDirect

Journal of Inorganic Biochemistry

journal homepage: www.elsevier.com/locate/jinorgbio

Metallation pathway of a plant metallothionein: *Cicer arietinum* MT2

Alma Salim[a], Serge Chesnov[b], Eva Freisinger[a,*]

[a] Department of Chemistry, University of Zurich, Zurich, Switzerland
[b] University of Zurich/ETH Zurich, Functional Genomics Centre Zurich, Zurich, Switzerland

ARTICLE INFO

Keywords:
Metallothionein
Cadmium
Metallation pathway
ESI-MS
Metal-thiolate cluster
Cicer arietinum

ABSTRACT

The plant metallothionein 2 protein from *Cicer arietinum* (cicMT2) is a typical member of the plant MT subfamily p2 that is characterized by an N- and C-terminal cysteine- (Cys-)rich, metal binding sequence connected by a long cysteine-free linker region. cicMT2 coordinates up to five Zn^{II} or Cd^{II} ions by its 14 cysteine thiolate groups forming a single metal-thiolate cluster. While MTs from other phyla are considerably well-studied, many details about plant MTs are missing. In this study the metallation pathway of cicMT2 is investigated using mass spectrometry. To evaluate the influence of the linker region as well as the interplay of the two Cys-rich stretches, the full-length cicMT2 protein as well as the individual Cys-rich domains with and without the linker region were analysed. Up to three Cd^{II} ions can be coordinated by the eight Cys residues of the N-terminal part and up to two Cd^{II} ions by the six Cys residues of the C-terminal sequence. However, no preferential binding to either of the two sequences is observed, which is in-line with the closely similar apparent binding constants of the individual domains obtained from competition reactions with the chelator 1,2-bis(2-amino-5-fluorophenoxy)ethane-N,N,N′,N′-tetraacetic acid. The combination of limited proteolytic digestion, mass spectrometry, dynamic light scattering, size-exclusion chromatography, and ^{19}F NMR spectroscopy enables us to draw conclusions about the overall protein-fold and the cluster formation process.

Significance

Metallothioneins are ubiquitously found in many organisms and play a pivotal role in metal ion homeostasis and detoxification. In particular, submetallated species are considered crucial for effective function, but received little attention so far as they are largely unstructured and tedious to handle. Here, we show that the metallation of a plant metallothionein is non-cooperative, ensuring that upon submetallation only low amounts of unstructured apo-species that are prone to proteolytic degradation exist. Results also reveal that the enigmatic linker region of plant metallothioneins only plays a subordinate role in metal-thiolate cluster formation as clusters will also form between the separate, non-linked domains.

1. Introduction

Plant growth, development, as well as survival depend on a multitude of internal and external factors [1,2]. The storage, transport, and homeostasis of essential metal ions such as Zn^{II} and Cu^{I}, as well as the detoxification of toxic metal ions such as Cd^{II}, Hg^{II}, Pb^{II}, or Ag^{I} is carried out, among others, by metallothioneins (MTs), a superfamily of small (< 10 kDa) cytosolic, cysteine-rich, and metal ion coordinating proteins [3–8]. MTs preferentially bind d^{10} metal ions, which are then arranged in thermodynamically stable metal-thiolate clusters [9]. The extraordinary high Cys content and the fact that the thiolate groups reside in the reduced state within these cluster structures suggest an additional protective function against reactive oxygen species (ROS), resulting in the formation of disulfide bridges and consequently metal ion release [10–13]. As MTs are generally devoid of secondary structural elements they are largely unstructured and highly flexible in the metal-free (apo) or submetallated state. Generally, only fully metallated species achieve a three-dimensional fold, that might - or not - impose sufficient rigidity to allow for structural investigations by NMR spectroscopy or X-ray crystallography.

Cicer arietinum (chickpea) metallothionein 2 (cicMT2) belongs to the plant MT subfamily p2. The main characteristic of this as well as of the p1 and p3 subfamilies of plant MTs, is the presence of N- and C-terminal Cys-rich sequences that are separated by a rather long Cys-free linker region. Predictions reveal that these regions contain secondary structural elements (mainly β-sheets) that were further analysed experimentally for cork oak MT2 and chickpea MT1 using CD, IR, and Raman spectroscopy [14,15]. The N-terminal region of cicMT2 contains eight

* Corresponding author.
E-mail address: freisinger@chem.uzh.ch (E. Freisinger).

https://doi.org/10.1016/j.jinorgbio.2020.111157
Received 27 February 2020; Received in revised form 18 June 2020; Accepted 21 June 2020
Available online 24 June 2020

```
                    1                   27              44    45              60                  78
                    |                   |               |     |               |                   |
cicMT2              SCCGGNCGCGSSCKCGSGCGGCKMYPDMSYTEQTTSETLVMGVA     SGKTQFEGAEMGFGAENDGCKCGSNCTCNPCTCK
N2                  SCCGGNCGCGSSCKCGSGCGGCKMYPD
C2                                                                   ENDGCKCGSNCTCNPCTCK
N-TEV-C_cicMT2   GSSCCGGNCGCGSSCKCGSGCGGCKMYPDMSYTEQTTSETLVMGVAENLYFQSGKTQFEGAEMGFGAENDGCKCGSNCTCNPCTCK
N1                  SCCGGNCGCGSSCKCGSGCGGCKMYPDMSYTEQTTSETLVMGVA
C1                                                               SGKTQFEGAEMGFGAENDGCKCGSNCTCNPCTCK
```

Fig. 1. Amino acid sequences of constructs. Cys residues are highlighted in black, the TEV cleavage site in construct N-TEV-C_cicMT2 is underlined and marked in gray. See text for details.

and the C-terminal region six cysteine residues as characteristic for all plant MT2 proteins, and the separating linker region has a length of 41 amino acids. Together, all Cys residues can coordinate up to five divalent metal ions *in vitro* leading to the formation of a single metal-thiolate cluster with a hairpin-like arrangement of the protein backbone [16].

The aim of this work is to study the metallation pathway of cicMT2 with Cd^{II} ions, which has never been performed for any plant MT so far. Studies of the metallation pathway are of special interest as recent findings indicate that generally MTs occur sub-metallated *in vivo* [17]. Ideally, such a study should identify the individual binding sites for each metal ion equivalent added to the protein during the folding process. While NMR spectroscopy using a specific labelling scheme could be a viable method for this purpose [18], it is not applicable for the plant MT1, MT2, and MT3 forms studied so far: Firstly, due to the general low abundance of secondary structural elements the fold of MTs is highly dependent on metal ion coordination. Hence sub-metallated species as occurring during a (non-cooperative) metallation process can be expected to be largely unstructured and thus highly flexible, resulting in peak broadening or even complete disappearance of signals. Secondly, as already the fully-metallated, and hence the presumably most structured, species of the mentioned plant MT forms did not yield any meaningful NMR spectra so far, tackling the metallation process with NMR is unfortunately completely unrealistic.

Accordingly, for the metallation studies described herein we are restricted to the identification of the respective Cys-rich region (N- or C-terminal), to which binding of each subsequently added metal ion equivalent occurs. We showed previously, that limited proteolytic digestion of Cd_5cicMT2 with *Tritirachium album* proteinase K leads to cleavage of the linker region at multiple sites but not within the Cys-rich regions, and that the assembly consisting of the single metal-thiolate cluster and the N- and C-terminal Cys-rich regions remains intact during size exclusion chromatography [16]. Subsequent analysis of the cleaved construct with MALDI-TOF spectrometry led to the dissociation of the cluster and only the metal-free peptide fragments were detected, due to the experimental conditions used (pH, ionization voltage) [16,19]. Hence for the present study the more gentle method of electrospray ionization mass spectrometry (ESI-MS) will be used for the study of the cleavage products, which can be applied at and above physiological pH to preserve the Cd^{II}-thiolate bonds. The potential of ESI-MS to determine metal ion-to-protein stoichiometries of MTs has been shown in several studies [20–22]. In particular, also the cooperative and non-cooperative binding of Zn^{II}, Cd^{II}, and As^{III} to the human MT_1a isoform as well as the stepwise metallation of the isolated β- and α-domains were successfully analysed [23–26]. Using a combination of N-ethylmaleimide labeling and tandem mass spectrometry experiments the removal of Cd^{II} from human MT_2A was investigated [27,28].

The general strategy followed here will thus be the stepwise addition of Cd^{II} ions to full-length cicMT2 followed by limited proteolytic digestion and analysis of the fragments with ESI-MS to identify metal ion binding to the respective Cys-rich regions. For comparison, also metal ion coordination to the individual Cys-rich regions will be investigated using the separately prepared peptides and hence avoiding the additional digestion step. To reduce the number of protease cleavage sites (that are located in the linker) and also to investigate a potential influence of the linker region on the metal ion binding preferences of the Cys-rich regions, another cicMT2 construct was produced that contains an artificial tobacco etch virus (TEV) protease cleavage site roughly in the center of the linker region. Results obtained with this construct will be compared to the respective separately prepared longer N- and C-terminal peptides (see Fig. 1). Identification of the binding region for each metal ion is complemented and corroborated by informations obtained from size exclusion chromatography, dynamic light scattering (DLS), and ^{19}F NMR spectroscopy.

2. Experimental procedures

2.1. Chemicals and solutions

The enzymes and purification systems used for plasmid construction were purchased from Promega AG (Dübendorf, Switzerland), and Sigma-Aldrich (Buchs, Switzerland). All buffers and chemicals were ACS grade or comparable from Sigma-Aldrich (Buchs, Switzerland), Biosolve (Sarl, France), Fisher Bioreagents (Reinach, Switzerland), and Chemie Brunschwig (Basel, Switzerland). Plasmid pRK793 for the production of TEV protease in *Escherichia coli* was a gift from David Waugh (Addgene plasmid # 8827) [29]. Rabbit liver MT2 from Enzo Life Sciences AG (Lausen, Switzerland) was a gift from Milan Vašák. All solutions were prepared using Millipore water and were degassed under vacuum. If necessary, solutions were saturated with argon.

2.2. Description of constructs

Full-length cicMT2 was obtained from the previously generated vector pGtMT2 [30]. The construct encoding the N-TEV-C_cicMT2 protein (see Fig. 1) was designed by introducing a TEV protease recognition site (ENLYFQ) into the linker region before residue Ser45. For the study of the separate N- and C- terminal domains two different sets of peptides were designed. The first set is based on the N-TEV-C_cicMT2 construct with the N-terminal peptide comprising residues Ser1-Ala44 (denoted N1) and the C-terminal peptide residues Ser45-Lys78 (C1). The second set represents the shorter peptides that are obtained experimentally after cleavage of full-length cicMT2 with proteinase K, *i.e.* residues Ser1-Asp27 (N2) and Glu60-Lys78 (C2), as described previously (Fig. 1) [16]. All coding sequences were cloned into the pGEX-4T-1 vector (GE Healthcare, Uppsala, Sweden) using the BamHI and *Xma*I restriction sites, which results in expression of proteins with a thrombin-cleavable N-terminal glutathione S-transferase (GST) tag. However, as we aim to generate proteins that carry their native N-terminal amino acid, an additional TEV protease cleavage site was introduced between the thrombin cleavage site and the respective coding protein sequence for all constructs used. The only exception is the N-TEV-C_cicMT2 construct, which already possesses a TEV cleavage site in the linker region (see above), and therefore here only the vector derived thrombin cleavage site was included in the sequence of the fusion protein. For the complete vector sequences see the Suppl. Mat.

2.3. Protein/peptide expression and purification

All constructs were recombinantly expressed in the *E. coli* strain BL21. Cells from a glycerol stock stored at −80 °C were grown at 37 °C overnight in lysogeny broth (LB) medium containing 100 μg/mL ampicillin (LB^{amp+}). Overnight precultures were diluted 1:100 into LB^{amp+} and incubated at 37 °C until an OD_{600} of 0.8. Expression was induced with 1 mM isopropyl-β-D-thiogalactoside and cells were grown for 6–8 h at 30 °C. Cells were harvested by centrifugation and stored at −80 °C for further use.

Cell pellets were resuspended in 1× phosphate-buffered saline (PBS; 10 mM Na_2HPO_4, 1.8 mM KH_2PO_4, 140 mM NaCl, 2.7 mM KCl, pH 7.3), lysed by ultrasonication and centrifuged. The respective supernatant was filtered through a 45 μm polyethersulfone filter (Sarstedt AG, Sevelen, Switzerland) and applied to a GST affinity column (GSTPrep FF 16/10, GE Healthcare). The column was first washed with 50 mL 1× PBS buffer containing 10 mM ethylenediaminetetraacetic acid (EDTA) (pH 8), and then with 100 mL 1× PBS buffer. Fusion peptides were stripped from the column using 5 mL of 50 mM Tris-HCl pH 8 supplemented with 50 mM reduced glutathione (GSH), and fractions were collected based on UV absorption at 280 nm. GSH was removed by overnight dialysis against 2 L of 50 mM Tris-HCl buffer with a pH of 8 for constructs cicMT2 and N-TEV-C_cicMT2 and 9 for N1, N2, C1, and C2, depending on the respective isoelectric point (pI). All constructs except N-TEV-C_cicMT2 were cleaved with 1 mg TEV protease (in 25 mM $Na_2HPO_4{\cdot}H_2O$, 100 mM NaCl, 10% glycerol, and 2 mM dithiothreitol, pH 7.5) per 40 mg of fusion protein overnight at room temperature followed by removal of the GST tag and TEV protease by size exclusion chromatography (SEC) using a HiLoad 16/60 Superdex 75 pg column (GE Healthcare) for cicMT2 or the respective 30 pg column for the N- and C-terminal peptides in 10 mM ammonium acetate, pH 7.4 or 9, again depending on the pI value. The N-TEV-C_cicMT2 fusion protein was cleaved with 1 unit thrombin per mg of protein in 50 mM Tris-HCl pH 8, for 20 h at room temperature and the GST tag was removed by SEC (HiLoad 16/60 Superdex 75 pg column) in 10 mM ammonium acetate pH 7.4. Eluted fractions of all protein and peptide constructs were lyophilized.

2.4. Preparation of apo-protein forms

The metal-free or apo-forms of N-TEV-C_cicMT2 as well as of the peptide fragments were prepared by dissolving the respective lyophilized protein in a buffer containing 10 mM Tris-HCl, pH 7.5 (pH 6.8 for the N2 and C2 peptides), 50 mM NaCl, 25 mM Tris(2-carboxyethyl) phosphine hydrochloride (TCEP) and 20 mM EDTA. For the preparation of apo-cicMT2 50 mM Tris-HCl, pH 8, and 10 mM $CaCl_2$ as required for subsequent cleavage with proteinase K was used. All proteins were purified by SEC using a Superdex Peptide 10/300 GL column (GE Healthcare) and the different buffers as indicated above depending on the protein/peptide. All solutions were vacuum degassed and argon saturated, and all steps were performed under strictly anaerobic conditions. For ESI-MS analyses, samples were desalted using C18 Zip Tips (Millipore, Billerica, MA, USA) and 0.1% formic acid in 50% acetonitrile at pH 2–3 for elution.

2.5. Cd^{II}-binding capacity of the terminal peptides

All titrations were performed inside an anaerobic chamber equipped with a palladium catalyst and filled with a 5% hydrogen/95% nitrogen gas mix (Coy Lab, Michigan, USA). The freshly prepared apo-peptides were titrated with incremental amounts of $CdCl_2$ (0–4 eq.) using separate solutions for each titration step. In addition, 1:1 mixtures of N1/C1 and N2/C2 were mixed with 0–6 eq. of Cd^{II} ions. After each metal ion addition a UV/Vis spectrum in the range of 200–600 nm was recorded on a Cary 60 scan spectrophotometer (Agilent Technologies AG, Basel, Switzerland) using a scan speed of 600 nm/min. Additionally, each of the four terminal peptides was oversaturated with Cd^{II} ions (5–6 eq.), passed through the SEC Superdex Peptide 10/300 GL column to remove unbound metal ions, and analysed by ESI-MS to confirm the maximum Cd^{II} binding capacity of the respective peptide.

2.6. Cd^{II} metallation pathway analysis

The apo-forms of the two full-length proteins, of the four separate terminal peptides as well as of the 1:1 mixtures of N1/C1 and N2/C2 were incubated with 0–5 eq. of Cd^{II} ions in the presence of 5 mM TCEP (pH 7). In addition, each N-TEV-C_cicMT2 sample was incubated with TEV protease (1 mg TEV protease: 20 mg protein), that was prepared as described before [31] with some modifications [32] in 10 mM Tris-HCl pH 8, and 50 mM NaCl buffer overnight at room temperature and each cicMT2 sample was digested with proteinase K using a molar ratio of 5:2 for 2 h at 28 °C in 50 mM Tris-HCl pH 8 and 10 mM $CaCl_2$. After metal ion addition, all samples were applied to the Superdex Peptide 10/300 GL column using 10 mM Tris-HCl, pH 7.5 or 6.8 for N2 and C2, and 50 mM NaCl as running buffer. Digested samples were desalted using C18 Zip Tips and 10 mM NH_4Ac in 50% MeOH, pH 7.5 for elution. Subsequent analysis was performed by ESI-MS at pH 7 to evaluate Cd^{II}-binding to the respective Cys-rich regions and fragments.

2.7. DLS of cicMT2

Small aliquots of cicMT2 loaded with different equivalents of Cd^{II} ions were taken prior to digestion with proteinase K, centrifuged for 10 min, and analysed by DLS (DynaPro Titan, Wyatt Technology). In addition, a sample of Cd_5N-TEV-C_cicMT2 was investigated. Each DLS analysis was performed with 20 μL of a 100 μM protein solution at room temperature, using 10 acquisitions with 5–10 s acquisition time each, and a laser power between 20 and 100%. The average hydrodynamic radius of each sample was obtained by curve fitting with the provided Dynamics software.

2.8. Determination of Cd^{II} binding constants by ^{19}F NMR

^{19}F NMR spectra were recorded on a Bruker AV2-400 MHz spectrometer with a 90 MHz spectral width, a 0.73 s acquisition time, and a 2 s pulse repetition rate. The respective protein and peptide concentrations in all samples were adjusted to result in Cd^{II} ion concentrations in the 130–350 μM range. As competitive chelator, 2.5 mM 1,2-bis(2-amino-5-fluorophenoxy)ethane-N,N,N′,N′-tetraacetic acid (5F-BAPTA) was used in 10 mM Tris-HCl, pH 6.8 or 7.5, and the ionic strength was 50 mM at 25 °C. To ensure that the equilibrium was reached, measurements were performed after 15 h incubation time. Binding constants were calculated according to Hasler et al. [33]. Exact metal ion concentrations in the samples were measured by flame atomic absorption spectroscopy. For the calculation, initial value for the Cd^{II}-5F-BAPTA binding constant of log $K_{Cd(BAPTA)}$ 11.75 [34] was adjusted to 50 mM ionic strength with the Chelator program [35] resulting in binding constant of log $K_{Cd(BAPTA)}$ 11.73 or $5.37{\cdot}10^{11}$ M^{-1}. Rabbit liver Cd_7MT2 was used as a control. Apparent binding constants were determined after 30 min, 1 h, 2 h, 4 h, 8 h, and 12 h incubation under the same conditions.

2.9. ESI-MS and MALDI mass spectrometry

All samples were analysed on a Synapt G2 quadrupole time-of-flight spectrometer (Waters, UK). Electrospray parameters were capillary 2.7 V, cone 50 V, and source temperature 80 °C. MS scans were accumulated and further processed with the software MassLynx 4.1 (Waters,

UK). Due to some limitations of the MaxEnt Software for complex mixtures of peptides with various masses, no deconvolution was performed for the experiment with proteinase K cleaved cicMT2. In this case, the quantitative analysis was performed based on the intensities of the doubly charged ions.

Cd_5cicMT2 cleaved with proteinase K and purified over SEC was analysed with matrix assisted laser desorption/ionization mass spectrometry (MALDI-MS). For MALDI-MS, the samples were desalted using C_{18} ZipTips (Millipore, Billerica, MA, USA) and spotted onto the MALDI target (MTP 384 target polished steel TF, Bruker Daltonics, Bremen, Germany) with 2 μL of α-Cyano-4-hydroxycinnamic acid (α-*CHCA*) solution in acetonitrile/water/trifluoroacetic acid (50:50:0.1) for subsequent MALDI-TOF measurements. The concentration of α-*CHCA* was 5 mg/mL.

MALDI measurements were performed on an ultrafleXtreme MALDI-TOF/TOF mass spectrometer equipped with a smartbeam laser (Bruker Daltonics). The measurement parameters were programmed in flexControl (Version 3.4): laser frequency of 1000 Hz in the positive reflector mode with acquisition ranging from 700 to 5000 Da. Final spectra consisted of 1000–3000 shots per analysis. MS and MS/MS data of ions of interest were acquired manually. The mass spectrometer was calibrated in MS mode for every new set of samples; in the MS/MS mode, the precursor ion was used as the reference mass in the individual analysis. Detected peptides were identified using high energy fragmentation technique. In this investigation, MS/MS data were acquired using MALDI LIFT TOF/TOF mass spectrometry in the positive ion mode. The fragmentation was induced by the smartbeam laser without use of collision gas. Precursor ions were then accelerated and selected in timed ion gate. In the LIFT cell, the fragment ions were further accelerated and the MS/MS data recorded. The assignment of the peptides and their fragments to the protein sequence was performed using the BioTools software (Bruker Daltonics).

3. Results and discussion

3.1. Binding capacity of the terminal peptides

3.1.1. Metal ion titrations monitored with UV spectroscopy

The apo-forms of the four terminal peptides were titrated with increasing amounts of Cd^{II} ions, and the increase of the S → Cd^{II} ligand-to-metal charge transfer (LMCT) band at 250 nm was monitored with UV spectroscopy (Fig. 2). The maximum absorptivity of peptides N1 and N2 is reached after addition of three Cd^{II} ions. For the C-terminal peptides C1 and C2 the maximum is reached when two Cd^{II} ions are added.

In all titrations, a red-shift of the LMCT bands can be observed that is indicative for the formation of a cluster structure [36–38], and hence the transition of some of the initially terminal thiolate ligands, that are mostly contributing to the absorptivity at 250 nm, into ligands that bridge two metal ions. Those bridging thiolate ligands give rise to the red-shifted LMCT bands in the roughly 260–270 nm range. The red-shift upon cluster formation can be accentuated by plotting the ratio $\varepsilon_{250nm}/\varepsilon_{265nm}$ against the number of Cd^{II} equivalents added, and the transition point is approximately the maximum/intersection of the first two linear fits per plot (Fig. 3) [39]. For both terminal peptides N1 and N2, this intersection is observed when 1.5 equivalents of Cd^{II} are added, and for the second equiv. the absorptivity increase at 265 nm gains in importance (Fig. 3A). Considering that the N-terminal domain features eight Cys residues that could in theory accommodate two separate tetrahedral $CdCys_4$ sites, this indication for an early onset of cluster formation is surprising. The further analysis of this finding would require additional (structural) investigations. Both C-terminal peptides behave like expected. The maximum is reached with the addition of one equiv. of Cd^{II}. Further addition of metal ions to this six Cys residues containing domain would require cluster formation, which is indeed evident from the decreasing $\varepsilon_{250nm}/\varepsilon_{265nm}$ ratio (Fig. 3B).

3.1.2. Mass spectrometry

ESI-MS spectra confirm the maximum Cd^{II} binding capacity for the two N-terminal peptides (Cd_3N1, M_r(obs) 4689.33 Da, M_r(calc) 4692.16 Da; Cd_3N2, M_r(obs) 2858.96 Da, M_r(calc) 2861.21 Da) as well as for C2 (Cd_2C2, M_r(obs) 2203.43 Da, M_r(calc) 2205.04 Da), while also showing some submetallated species (Fig. 4). For peptide C1, however, next to the signal of the Cd_2-species (Cd_2C1, M_r(obs) 3701.61 Da, M_r(calc) 3703.67 Da), also an intensive signal for a Cd_3 species (Cd_3C1, M_r(obs) 3813.0 Da, M_r(calc) 3816.08 Da) is observed and in addition, signals that indicate dimer-formation with four ($Cd_4(C1)_2$, M_r(obs) 7399.2 Da, M_r(calc) 7407.35 Da) and five Cd^{II} ions ($Cd_5(C1)_2$, M_r(obs) 7512.2 Da, M_r(calc) 7519.75 Da) are detected. Although this dimerisation of the separate C-terminal domain is probably not physiologically relevant, it is interesting from a coordination chemistry point of view. Considering the ratio of five Cd^{II} ions to just 12 Cys ligands, it is clear that some sort of cluster structure must be present that is connecting the two peptides, and that the number of bridging thiolate groups in this arrangement must be quite high. An inorganic model compound with five Hg^{II} ligands and 12 coordinating thiolate groups, in which each Hg^{II} ion shows a tetrahedral tetrathiolate environment is known from the literature [40], but any such compound would be unprecedented for MTs or other biological systems. Hence, a structural model is difficult to propose, especially considering the smaller ionic radius of Cd^{II} compared to Hg^{II}, being unfavourable for a highly bridged structure.

Why is the higher coordination number not evident from the increase of the LMCT band in the UV spectra?

On the one hand, only small changes are expected, considering (i) 2 Cd^{II} ions per C1 peptide for a Cd_2C1 species *versus* 2.5 Cd^{II} per C1 in the $Cd_5(C1)_2$ dimer and (ii) that for coordination of additional Cd^{II} ions terminal thiolates are transformed into bridging thiolates, which have a relatively small effect on the LMCT band. On the other hand, a highly bridged, well-ordered cluster structure should lead to a bathochromic shift of the LMCT bands as particularly observed for the N-terminal, but less for the C-terminal peptides. Accordingly, it can be also hypothesized that, due to steric reasons, there is either not a pure Cd-thiolate cluster and other ligands, *e.g.* carboxylates of Glu and Asp, complete the Cd^{II} coordination spheres, or that some of the coordination sites are vacant or in fast exchange (share ligands) as recently shown for a bacterial MT from *Pseudomonas fluorescens* [32]. The highly metallated Cd_3C1 species can be explained as an artificial adduct species generated when the $Cd_5(C1)_2$ falls apart under ESI-MS conditions. It is unlikely that such a species could be specifically prepared by Cd^{II} addition to the C1 peptide.

Titration of the peptide mixtures with Cd^{II} ions shows incremental increase of the LMCT band at 250 nm up to five Cd^{II} ions for N2/C2, while the 1:1 mixture of N1 and C1 coordinates only four Cd^{II} ions by thiolate groups (Fig. 2). Apparent is again a red-shift of the LMCT bands in the N2/C2 mixture indicative for a bridged cluster structure. Again, rather early onset of cluster formation is observed based on the maximum value for the $\varepsilon_{250nm}/\varepsilon_{265nm}$ ratio at already two equiv. of Cd^{II}, indicating one isolated $CdCys_4$ site each in the N-terminal and the C-terminal peptide, respectively, and cluster formation thereafter (Fig. 3C).

3.2. Metallation pathway of cicMT2

3.2.1. Proteinase K cleavage of cicMT2

First, fully metallated cicMT2 (Cd_5cicMT2) was cleaved with *T. album* proteinase K and the cleavage products were analysed by MALDI-MS (Suppl. Material). In contrast to the previous study [16] only a 2.5-fold excess of protease was used. Detected peptides were subsequently sequenced with MALDI-MS/MS, and the fragment ions were aligned with the entire protein sequence as well as with the most likely fragments using the Bruker BioTools 3.2 software. In agreement with the previous results, selective cleavage resulting in N2 and C2 as well as in

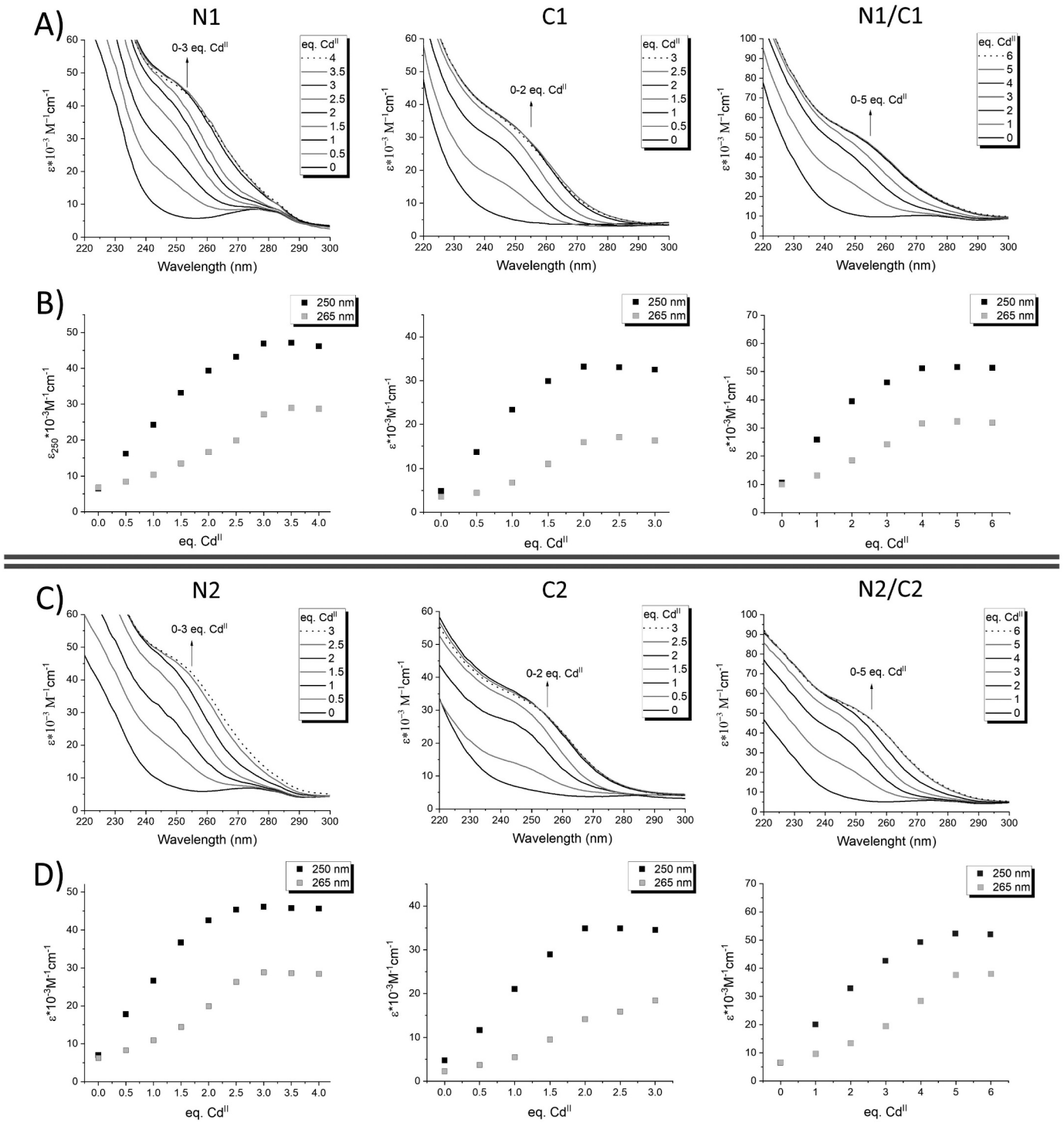

Fig. 2. UV spectra of the apo-protein form titrations with Cd^{II} ions (A and C), and plots of extinction values at 250 nm and 265 nm (B and D) for the indicated peptides as well as of the respective 1:1 mixtures.

two slightly shorter peptides (N2-short (1-23) and C2-short (61-78)) was observed.

The ESI-MS spectrum of proteinase K cleaved apo-cicMT2 at acidic conditions (pH 2) shows all N- and C-terminal peptides in the +2 charged state, *i.e.* observed *m/z* values are 1009.31 (N2-short), 1262.38 (N2), 925.82 (C2-short), and 990.34 (C2) (Fig. 5A). It should be noted, that the intensities of the N-terminal peptides are lower than the intensities of the C-terminal peptides in all spectra due to a better ionization of the latter in the ESI-MS experiments. Hence the signal intensity cannot be correlated to the respective peptide concentration in the sample. Subsequently, apo-cicMT2 was titrated with 1–5 equiv. Cd^{II} and ESI-MS spectra were recorded at physiological pH (Fig. 5B–F) as well as at pH 2 in order to differentiate Cd^{II}-bound peptides from non-coordinating linker fragments (data not shown). Based on the +2 charge states of the observed peptide fragments a mass increase by 56 Da relative to the apo-peptide fragment is indicative for the chelation of one Cd^{II} ion. However, as the background noise of the spectra in Fig. 5 is rather high due to side-products from unspecific cleavage and the presence of smaller fragments from the linker region, assignment of the different N-terminal species is not always unambiguous and

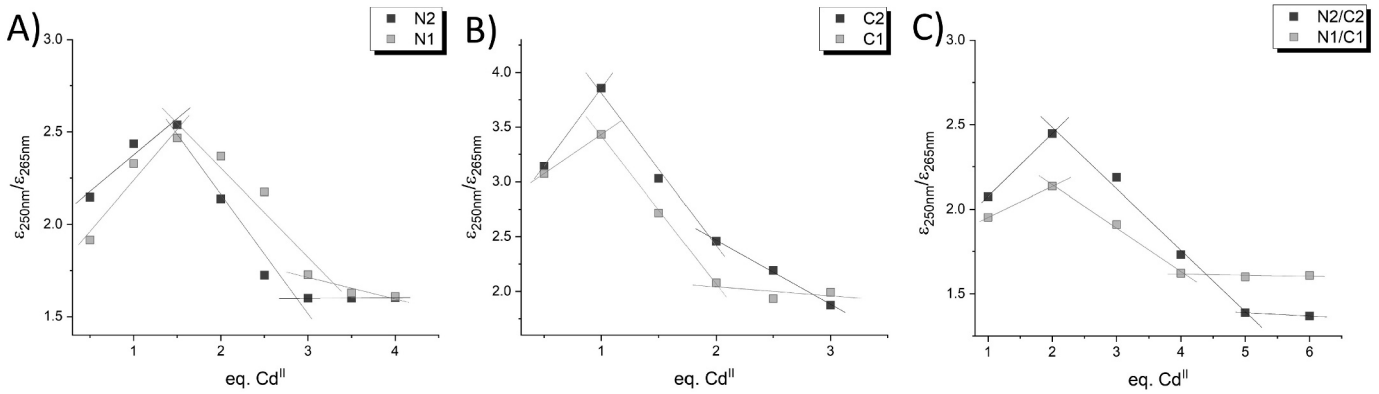

Fig. 3. Plots of the quotient of extinction values at 250 nm and 265 nm against the Cd^{II} equivalents added for A) N1 and N2, B) C1 and C2, as well as C) 1:1 mixtures of N1/C1 and N2/C2. Linear least-square fits for the respective areas are included to better visualize the trends.

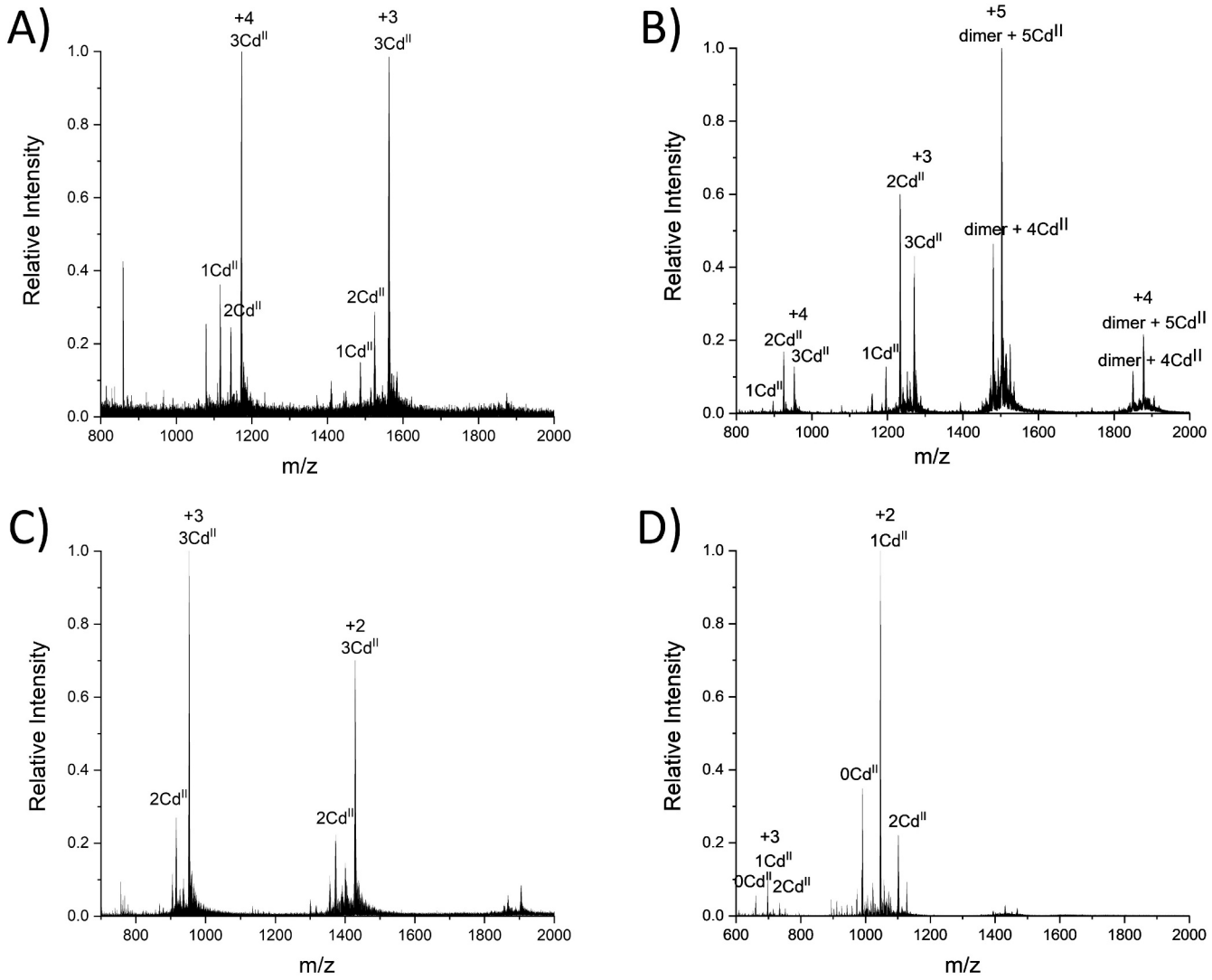

Fig. 4. Non-deconvoluted ESI-MS spectra of the four terminal peptides: A) Cd_3N1 ($M_{r(obs)}$ 4689.33 Da, $M_{r(calc)}$ 4692.16 Da), B) Cd_2C1 $M_{r(obs)}$ 3701.61 Da, $M_{r(calc)}$ 3703.67 Da), C) Cd_3N2 ($M_{r(obs)}$ 2858.96 Da, $M_{r(calc)}$ 2961.21 Da), and D) Cd_2C2 ($M_{r(obs)}$ 2203.43 Da, $M_{r(calc)}$ 2205.04 Da).

quantification of the smaller peaks is highly error prone. In addition, the masses of one of the linker fragments (YTEQTTSETL; Mr(calc) 1172.21 Da) and of Cd_3N2-short (Mr(calc) 1177.31 Da) are too close together to be resolved in separate peaks making quantification even more difficult. Hence, the metallation process of the N-terminal fragment can be monitored only qualitatively. Cleavage of Cd_1cicMT2 reveals roughly equally intense signals for the Cd_1- and Cd_2-forms of the N-terminal peptide fragments, while the intensity of the signals for the Cd_1-forms of the C-terminal peptide fragments is slightly higher than that for the Cd_2-forms (Fig. 5B). Only low amounts of apo-species are detected. The ESI-MS spectrum after cleavage of Cd_2cicMT2 is very similar and in addition, formation of a Cd_3N2 species can be observed

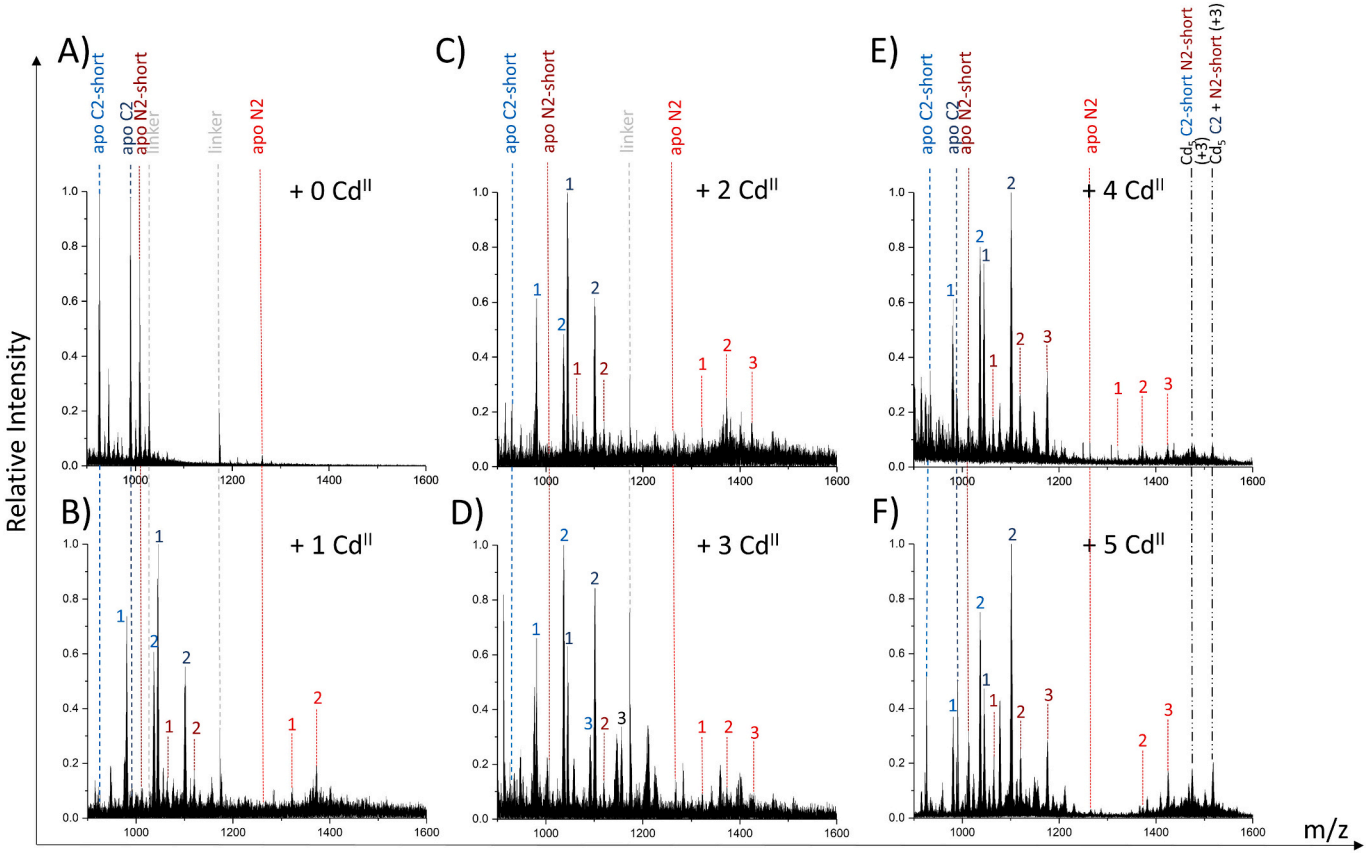

Fig. 5. Non-deconvoluted ESI-MS spectra of proteinase K cleaved cicMT2 samples upon stepwise metallation with 0–5 Cd^{II} ions. The numbers correspond to the equivalents of Cd^{II} bound to the respective peptide fragment. The color of the respective numbers corresponds to the color used for the labeling of the apo peptide forms.

(Fig. 5C). However, assignment of the Cd_3N2-short species is not unambiguously as discussed and hence a reliable quantification is not possible. A major change occurs for the Cd_3cicMT2 sample, as for the first time C-terminal Cd_3 species are observed, while the highest intensity is detected for the C-terminal Cd_2 species followed by the Cd_1 species (Fig. 5D). Again, formation of a Cd_3 species by the C-terminal peptides cannot be explained with the enigmatic Cd-thiolate clusters of MTs and further interpretations are highly hypothetic. An alternative view is the presence of an additional metal ion binding site not involving any thiolate ligands. An indication for the feasibility of this assumption is the observation of a Cd_6cicMT2 species reported earlier [41]. Also at this titration point, signals in-line with possible N-terminal Cd_3 species are observed, although quantification is again difficult due to the high signal-to-noise ratio in the respective region of the ESI-MS spectrum and the mentioned general low intensity of the signals of the N-terminal peptides. In the Cd_4cicMT2 and Cd_5cicMT2 samples assignment of N-terminal Cd_3 species is now unambiguous, because in contrast to the spectra after addition of 1–3 equiv. of Cd^{II}, no linker signal is detected in the spectra at pH 2. Disappearance of this signal is probably related to the altered fold of cicMT2 at higher metal ion load and accordingly to a different cleavage pattern. In contrast, the intensities of the C-terminal Cd_3 species are diminished. Most significantly, signals for peptide fragments that are joined by a metal-thiolate cluster are observed for the first time, that is for Cd_5(N2-short + C2-short) and Cd_5(N2-short + C2) (Fig. 5E, F). The reason why no clustering involving the N2 peptide is observed, might be again the general low intensity of that peptide in ESI-MS. The relative abundance of the C-terminal Cd_2 species remains high in both samples, suggesting that these species are relatively stable and favored by the C-terminal peptides.

3.2.2. 1:1 mixtures of N2 and C2

How important for the metallation pathway is the fact, that the N- and C-terminal Cys-rich regions are linked to each other? Does this influence the Cd^{II} binding preference to a specific domain? Is heterodimeric cluster formation still observed? To answer these questions, the same metallation experiment as performed for the full-length protein was also conducted with the separate Cys-rich domains, using the sequences for the peptides obtained after limited proteolytic digestion with proteinase K, *i.e.* N2 and C2. N2 and C2 are nearly devoid of residues originating from the linker region. The peptides were prepared separately, mixed in a 1:1 molar ratio, loaded with Cd^{II} ions, and passed through a Superdex Peptide 10/300 GL column for buffer exchange before ESI-MS analysis (Fig. 6). Compared to the digestion experiment with proteinase K described above, it is now possible to deconvolute the spectra and a considerable lower noise and less background signals are seen. This allows now also the analysis of the N-terminal species with higher reliability.

Spectra measured at acidic conditions show signals of both peptides with observed mass values of 1980.4 Da for C2, and 2524.49 Da for N2 (Fig. 6, + 0 Cd^{II}). The detected species in the spectra after addition of one and two Cd^{II} ions are very similar to those seen in the experiment with proteinase K cleavage (Fig. 5B, C). In both spectra, Cd_1 species of both peptides are observed as well as Cd_2 species of the N-terminal domain. Cd_2 species of the C-terminal domain only appear after addition of two equivalents of Cd^{II}. While after addition of the first Cd^{II} equivalent the Cd_1 species dominate for both Cys-rich regions and hence no binding preference to either domain is evident, the Cd_1:Cd_2 species ratio roughly inverses for N2, but not C2, when the second Cd^{II} ion is added. This indicates the preferential formation of Cd_2N2 over Cd_2C2 and hence a higher stability of the second metal ion binding sites

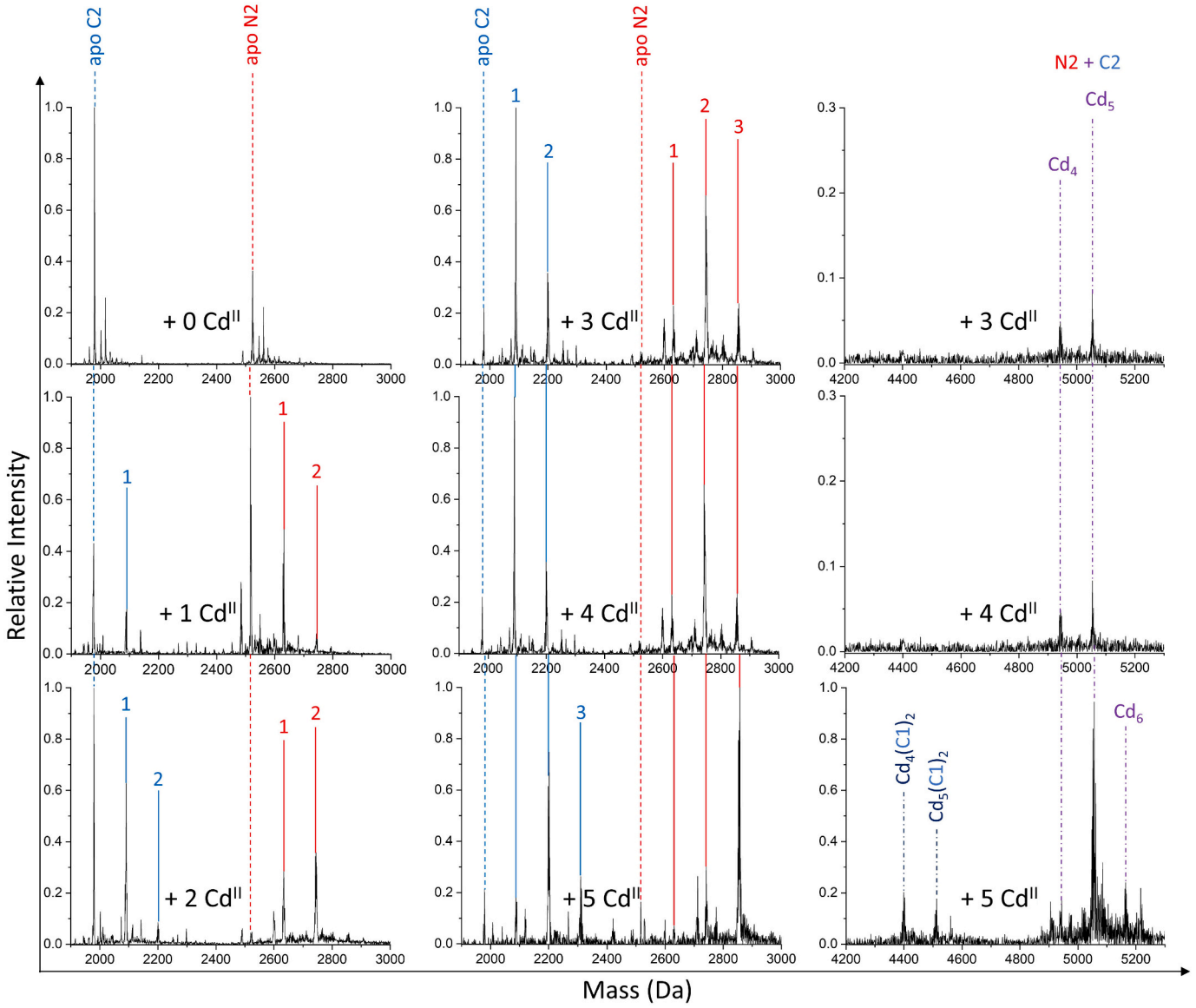

Fig. 6. Deconvoluted ESI-MS spectra of N2 and C2 terminal peptides upon stepwise metallation with 0–5 Cd^{II} ions. The color of the numbers assigned to the peaks corresponds to the color used for the labeling of the apo peptide forms.

in N2 compared to C2. As for full-length cicMT2, addition of three Cd^{II} ions shows the formation of an N-terminal Cd_3 species, but no Cd_3C2 species is detected (Fig. 6). For C2 the Cd_1 species has still the highest intensity. Hence binding of the third metal ion to N2 seems to be favored over C2. From this titration point on, signals for a Cd_4N2C2 (Mr (obs) 4945.87 Da, Mr(calc) 4954.74 Da) and Cd_5N2C2 cluster (Mr(obs) 5055.47 Da, Mr(calc) 5067.15 Da) can be detected. This shows clearly that cluster formation neither depends on the linker region nor does it require a covalent link between the two Cys-rich regions. Upon addition of five Cd^{II} ions also homo-dimers of the form $Cd_4(C2)_2$ (Mr(obs) 4401.16 Da, Mr(calc) 4410.08 Da) and $Cd_5(C2)_2$ (Mr(obs) 4512.00 Da, Mr(calc) 4522.49 Da) appear, which are clearly not physiologically relevant. In this spectrum also a Cd_3C2 species is observed for the first time, which again might indicate a third binding site in this peptide or represents an artifact when the Cd_5 cluster falls apart during ionization as discussed above. In addition, a low intensity signal for a Cd_6N2C2 species is detected (Fig. 6). Overall and in particular, the coordination of three Cd^{II} ions to the N-terminus clearly shows that shortening of the linker region does not reduce the binding capacity for divalent metal ions. A similar observation was reported for *Quercus suber* (cork oak) MT2 [14].

3.2.3. TEV cleavage of N-TEV-C_cicMT2

To increase cleavage specificity and to minimize the amount of fragments that were observed after proteinase K cleavage, a TEV protease recognition site (ENLYFQ) was introduced into the linker region of cicMT2 (Fig. 1). cicMT2 and N-TEV-C_cicMT2 show identical behavior in the Cd^{II} titration experiment followed by UV spectroscopy, and the binding capacity for five Cd^{II} ions is retained (Suppl. Mat.). The position of the cleavage site before position Ser45 was on the one hand chosen, because cleavage at the N-terminal site of a Ser residues has been shown to be highly efficient [42]. On the other hand, cleavage in roughly the center of the linker region adds half of its amino acids to each of the two resulting peptides and hence should minimize the effects of the missing linker on the metal ion binding properties of the terminal peptides. Initially it was planned to retain the GST fusion tag at the N-terminus during the experiments to enable separation of the otherwise similarly sized N- and C-termini by gel filtration after

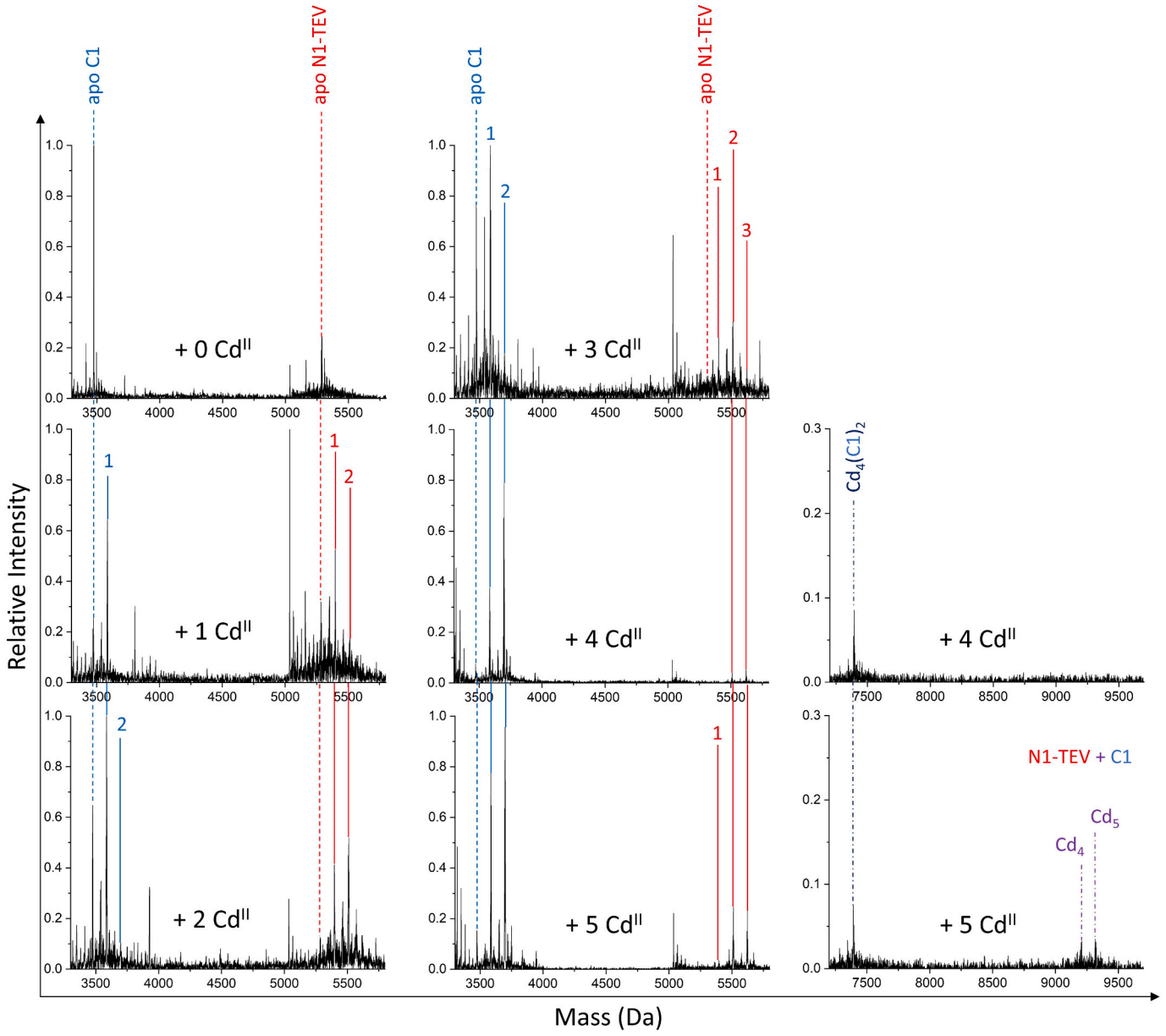

Fig. 7. Deconvoluted ESI-MS spectra of N-TEV-C_cicMT2 samples upon stepwise metallation with 0–5 Cd^{II} ions. The color of the numbers assigned to the peaks corresponds to the color used for the labeling of the apo peptide forms.

cleavage; however, initial experiments showed that GST significantly alters the metal ion binding properties of the peptide compared to the un-tagged protein. Therefore, the GST tag was removed *via* thrombin cleavage prior to the metallation experiments. As before, cleavage mixtures were analysed by ESI-MS. Results before addition of metal ions reveal two peptide fragments: N1 with the additional six amino acids of the TEV cleavage site (N1-TEV; Mr(obs) 5289.23 Da, Mr(calc) 5293.93 Da) and C1 (Mr(obs) 3475.33 Da, Mr(calc) 3478.85 Da) (Fig. 7).

After addition of one Cd^{II} equivalent, Cd_1 species of both peptides are observed, again confirming the absence of any preference for one domain over the other. In contrast to the proteinase K cleaved cicMT2 sample, no Cd_2C1 species is observed while again a Cd_2N1-TEV species is seen. Addition of two metal ions reveals again a larger signal of the Cd_2N1-TEV species compared to the Cd_1 form. No major changes compared to previous results are obtained for the metallation with 3–5 Cd^{II} ions, except that no Cd_3C1 species is observed in any of the spectra. Also homo-dimer formation of the C-terminal peptide is again observed after addition of four or five equivalents of Cd^{II} ($Cd_4(C1)_2$, Mr.(obs) 7397.64 Da, Mr.(calc) 7407.34 Da). Cluster formation between N1-TEV and C1, however, is only observed when five Cd^{II} ions are added to this construct. This delayed cluster formation is probably correlated to the six additional amino acid of the TEV cleavage site in the center of the linker region. Hence, the altered linker sequence seems to have an influence on the cluster formation ability of the protein.

3.2.4. 1:1 mixtures of N1 and C1

To evaluate the possibility that the six amino acids of the TEV cleavage site (ENLYFQ) in N1-TEV influence its metal ion binding abilities, N1 (residues 1–44) and C1 (45–78) were produced as separate peptides (Fig. 1). The ESI-MS spectrum of the mixture acquired at acidic conditions shows signals for both peptides, that is N1 (Mr(obs) 4346.1 Da, Mr(calc) 4354.93 Da) and C1 (Mr(obs) 3475.33 Da, Mr (calc) 3478.85 Da) (Fig. 8). Upon metallation, two significant changes compared to the N-TEV-C_cicMT2 construct can be seen. First, upon addition of the first Cd^{II} ion no formation of the Cd_2N1 species is

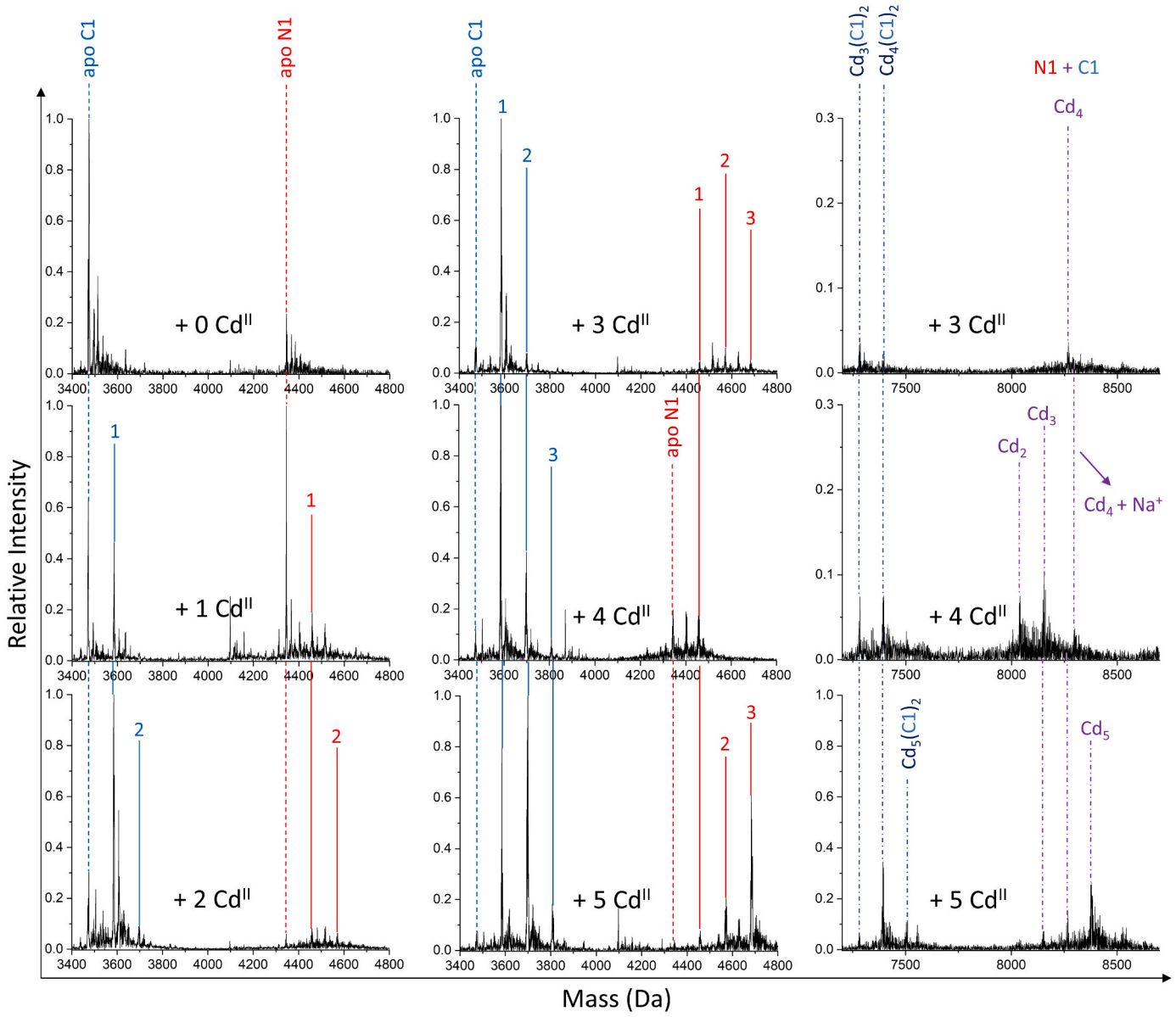

Fig. 8. Deconvoluted ESI-MS spectra of N1 and C1 terminal peptides upon stepwise metallation with 0–5 Cd^{II} ions. The color of the numbers assigned to the peaks corresponds to the color used for the labeling of the apo peptide forms.

observed. Second, formation of a Cd_3C1 species is again detected when four or five Cd^{II} ions are added to the mixture. Cd_1C1 has the highest intensity of all species up to the addition of four Cd^{II} ions, while the Cd_2C1 species increases in intensity and becomes the major signal in the spectra after addition of five Cd^{II} ions (Fig. 8). In the same spectrum, and in agreement to the results with N-TEV-C_cicMT2, a Cd_5N1C1 species can again be observed (Mr(obs) 8381.67 Da, Mr(calc) 8395.83 Da) next to Cd_4- and $Cd_5(C1)_2$ homo-dimers. It is also intriguing that Cd_4N1C1 cluster formation is already observed upon addition of three Cd^{II} equivalents, and upon addition of four metal ions unprecedented formation of Cd_2- and Cd_3N1C1 species is observed next to the Cd_4N1C1 species, the origin of it not being clear.

3.2.5. *Evaluation of cooperative behavior and influence of the linker region on cluster formation*

A summary of the results obtained with the proteolytically cleaved full-length constructs cicMT2 and N-TEV-C_cicMT2, as well as with the 1:1 mixtures of the separate peptides N1/C1 and N2/C2, is presented in Fig. 9 (tables with values are given in the SI). Upon stepwise addition of Cd^{II} ions first formation of sub-metallated species is observed and hence the metallation proceeds in absence of positive cooperativity. Domain filling with positive cooperativity in place would result in a statistical underrepresentation of intermediate metallated states, hence, for example, after addition of one Cd^{II} equivalent (per domain or in total is not really crucial) a Cd_2N2 species would be already observed, but the Cd_1N2 form would be clearly diminished. This is obviously not the case. After addition of one Cd^{II} ion exclusively Cd_1N2 is, but no Cd_2N2 is detected (Fig. 9B). Addition of two Cd^{II} equivalents leads to the formation of Cd_2N2, but also considerable amounts of Cd_1N2 are still presence. Hence there is no positive cooperativity. On the other hand, Cd_2N2 is observed, but no Cd_2C2. However, N2 and C2 must be considered as completely independent (and even physically separated) protein domains, at least at lower Cd^{II} concentrations, and accordingly the preferential filling of the N-terminal domain with metal ions is not to be explained with cooperativity but with a higher binding affinity of the N-terminal domain for Cd^{II} at certain metal-to-protein ratios (see below). The same is true for the titration of the other three constructs (Fig. 9A, C, D). Accordingly, presence of intermediate metallated states

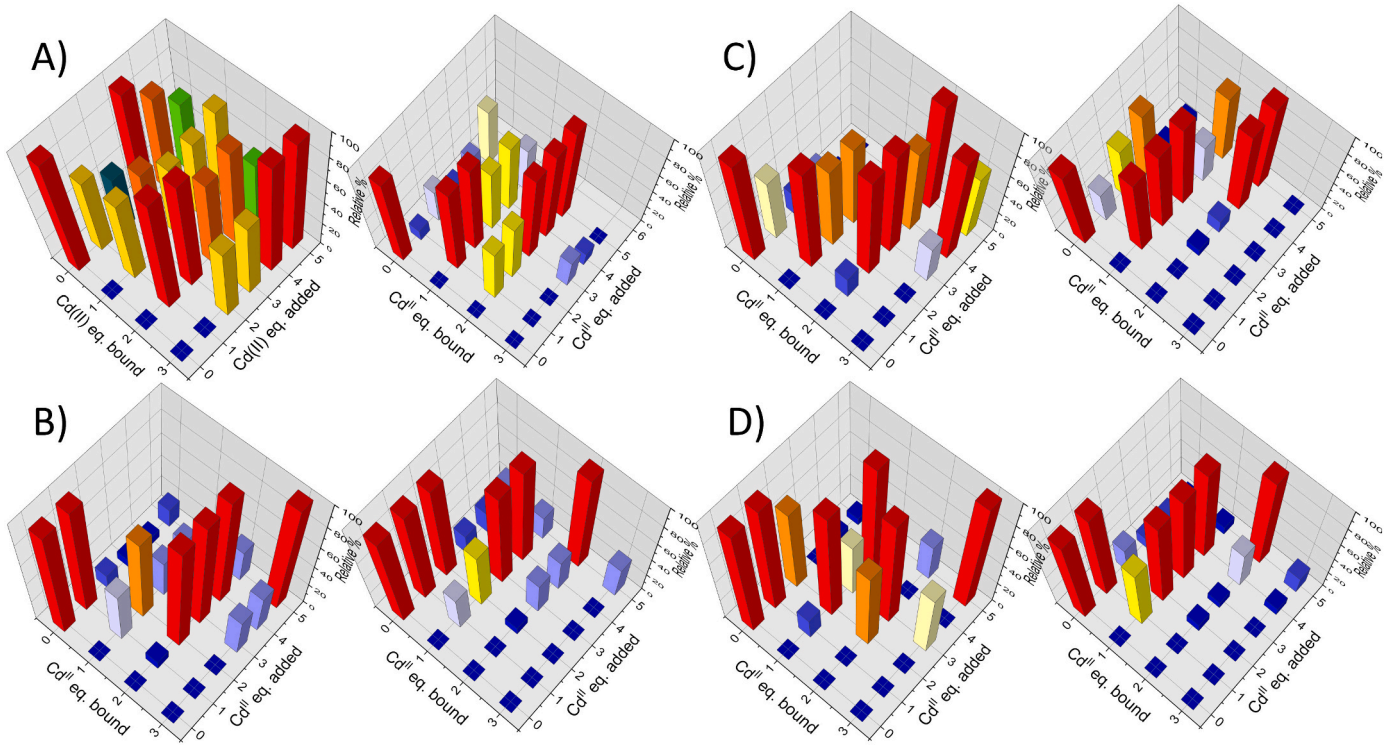

Fig. 9. Metallation of the N- and C-terminal Cys-rich regions as a function of Cd^{II} added to the solution. The relative percentage of a species is calculated for each peptide fragment separately with 100% referring to the highest peak of a given species in all spectra of a given titration with 0–5 equiv. Cd^{II}. The left graph of each part refers always to the N-, the right part to the C-terminal fragment. A) Proteinase K cleaved cicMT2, B) 1:1 mixture of N2/C2, C) TEV cleaved N-TEV-C_cicMT2, D) 1:1 mixture of N1/C1.

that become the most abundant species during the early and mid-stages of the Cd^{II} titration experiment suggests that this metallation pathway proceeds clearly in a noncooperative fashion [25]. From a thermodynamic point of view, the affinities for coordination of the first Cd^{II} ion to the N- or the C-terminal region are comparable, *i.e.* $K_{app}(Cd_1N1/N2) \approx K_{app}(Cd_1C1/C2)$. Binding of two Cd^{II} to the N-terminus is observed earlier than to the C-terminus and hence $K_{app}(Cd_2N1/N2) > K_{app}(Cd_2C1/C2)$. The reason for this might be just that the number of Cys residues in the N-terminal Cys-rich region is higher (8 Cys *versus* 6). In addition, $Cd_3N1/N2$ species are observed from addition of three equiv. of Cd^{II} on, and hence at a titration point where mostly $Cd_1C1/C2$ still prevails over $Cd_2C1/C2$. Accordingly it even seems that $K_{app}(Cd_3N1/N2) > K_{app}(Cd_2C1/C2)$.

While truncation of the linker region does not influence the binding capacity of the peptides, there seems to be an influence on the formation of the Cd_5NC cluster (Fig. 10). When the peptide mixtures are titrated with Cd^{II} ions, it is obvious from the UV spectra that the addition of more than two Cd^{II} equivalents causes the onset of some sort of cluster formation (Fig. 3C). This can be sufficiently explained with the formation of Cd_3N species as well as increasing amounts of Cd_2C species that both require bridging thiolate groups. Both species are observed in the respective ESI-MS spectra when three equiv. of Cd^{II} ions were added to the mixtures (Figs. 5 and 8). Nevertheless, while in addition already a small signal for a Cd_5N2C2 species is observed at this titration point, the Cd_5N1C1 species can be only detected when five equiv. of Cd^{II} are added to the N1/C1 mixture. Hence in the case of the separate terminal peptides, the presence of parts of the linker region seems to, at first glance, even hinder Cd_5NC cluster formation. Comparing this with the results obtained with the full-length proteins, ESI-MS spectra of the digested cicMT2 protein show a Cd_5 cluster involving the (partially

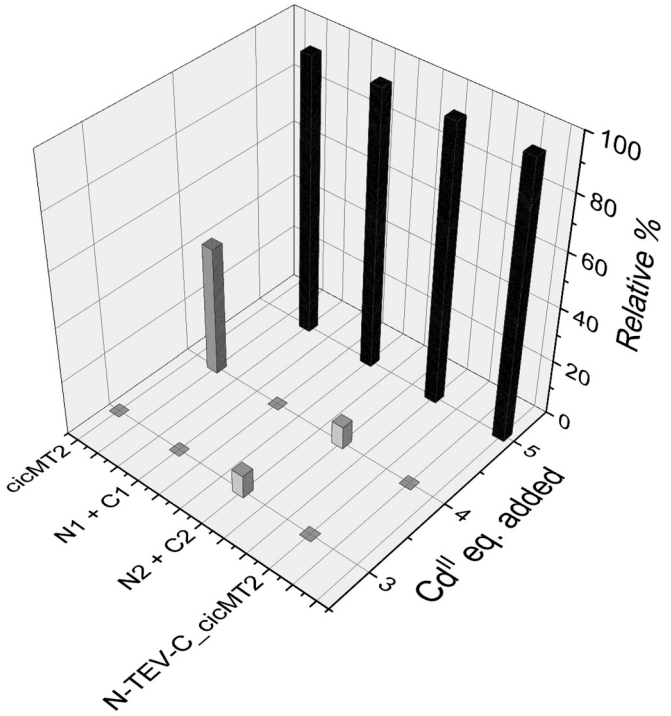

Fig. 10. Cluster formation of the type Cd_5NC as a function of Cd^{II} ion added to the solution.

Table 1
R_h and polydispersity (Pd) values obtained by DLS for the stepwise metallation of cicMT2 with Cd^{II} ions.

	R_h (nm)	Pd (%)
apo-cicMT2	3.02 ± 0.11	25.1 ± 2.8
Cd_1cicMT2	2.52 ± 0.07	12.9 ± 2.3
Cd_2cicMT2	2.33 ± 0.05	20.8 ± 1.4
Cd_3cicMT2	1.85 ± 0.04	25.6 ± 2.8
Cd_4cicMT2	1.66 ± 0.05	18.9 ± 2.3
Cd_5cicMT2	1.48 ± 0.04	26.2 ± 1.6
Cd_5N-TEV-C_cicMT2	1.60 ± 0.08	22.0 ± 1.7

even more shortened) N2 /C2 peptides when four Cd^{II} ions were added, while for the N-TEV-C_cicMT2 construct the Cd_5 cluster only appears in the spectra when five Cd^{II} ions were added. In addition to Cd_5 cluster formation, also Cd_4 clusters are observed, in particular in the N1/C1 and N2/C2 mixtures upon addition of three Cd^{II} ion.

3.3. Structure compaction upon stepwise metallation of cicMT2

As MTs are to the largest extent devoid of secondary structural elements, the folding heavily depends on metal ions [43–46]. Hence, the folding process of cicMT2 was studied by observing the changes in hydrodynamic radius (R_h) during the metallation process using DLS. The data show a gradual decrease in R_h and hence a compaction of the protein structure, from 3.02 ± 0.11 nm in apo-cicMT2 to 1.48 ± 0.04 nm in Cd_5cicMT2 (Table 1). The observed radius for the completely metallated protein (7.8 kDa for the protein part) is in good agreement to literature values of proteins with similar molecular weights: Aprotinin (6.8 kDa) has an R_h of 1.35 nm and cytochrome C (12 kDa) of 1.77 nm [47]. The largest changes of approximately 0.5 nm each are observed upon addition of the first and of the third Cd^{II} ion. Considering the R_h of 3.0 nm for the apo-protein and making the rough approximation that the N-terminal domain, the C-terminal domain and the linker contribute 1/3 each to the total amino acid chain length, contraction by 0.5 nm could be explained by folding of one domain (a hairpin formed by a 1 nm stretch should have a length of roughly 0.5 nm), contraction by another 0.5 nm by folding of the second domain (Fig. 11). Accordingly, upon addition of the first Cd^{II} ion, on average one domain folds around the metal ion resulting in a R_h of 2.5 nm. Only addition of a total of three Cd^{II} ions leads to the folding of the second

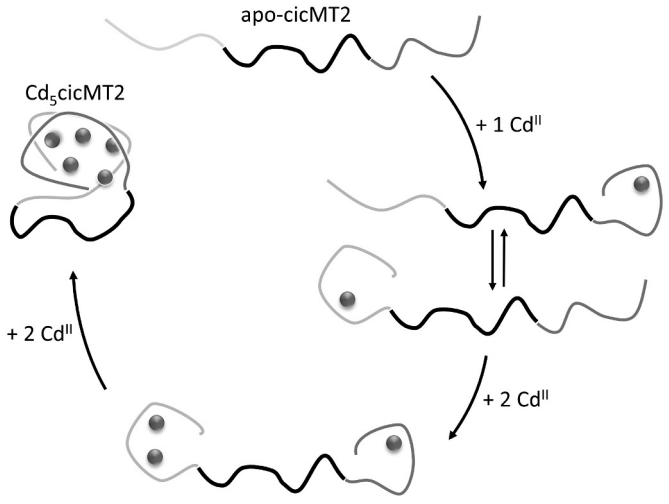

Fig. 11. Schematic representation of the folding pathway upon metal ion binding: light gray, N-terminal Cys-rich region; dark gray, C-terminal Cys-rich region; black, linker region; gray balls, Cd^{II} ions. Note that after addition of 1 Cd^{II} ion, both coordination to the N- as well as to the C-terminal part is observed.

Table 2
Apparent Cd^{II} binding constants (K_{app}) of the separate fully-metallated terminal peptides, the full-length cicMT2 protein, and rabbit liver MT2 as well as equivalents of Cd^{II} removed by competition with 5F-BAPTA.

	K_{app} [M^{-1}]	log (K_{app})	Cd^{II} eq. removed
Cd_3N2	5.30×10^{11}	11.71 ± 0.20	2.69 ± 0.03
Cd_2C2	1.79×10^{11}	11.25 ± 0.05	1.91 ± 0.01
Cd_3N1	5.80×10^{11}	11.76 ± 0.15	2.65 ± 0.01
Cd_2C1	9.84×10^{11}	11.99 ± 0.03	1.71 ± 0.01
Cd_5cicMT2	8.82×10^{11}	11.94 ± 0.28	4.43 ± 0.05
Cd_7MT2	2.79×10^{14}	14.44 ± 0.07	1.05 ± 0.08

domain, *i.e.* $R_h \sim 1.9$ nm. The fourth and fifth equivalents cause further compaction of the structure that is in accordance with Cd_5 cluster formation observed in ESI-MS now also involving the linker region, leading finally to a R_h of 1.5 nm, which is half the radius seen for the apo-protein. For comparison, the radius for Cd_5N-TEV-C_cicMT2 is with 1.6 nm slightly larger, which might reflect the slightly longer linker region in this construct.

3.4. Thermodynamic stability of Cd^{II} binding

5F-BAPTA is a fluorinated chelator that forms 1:1 complexes with divalent metal ions and was incubated with Cd_5cicMT2 as well as Cd_2C1/C2 and Cd_3N1/N2 as competing ligand to determine the apparent stability constants of the protein and peptides. The ^{19}F NMR spectra of the mixtures show in each case two main signals at −115 and −123 ppm (Fig. S5), which correspond to $Cd_1$5F-BAPTA and free 5F-BAPTA, respectively [48]. Peaks were integrated and the resulting concentrations used to calculate the apparent Cd^{II}-binding constants for each fully-metallated construct. Using the conditional stability constant of $Cd_1$5F-BAPTA of 5.37×10^{11} M^{-1} obtained with the program *Chelator* [35] for 50 mM NaCl, pH 7.5, apparent stability constants were calculated according to Hasler et al. [33] (Table 2, Data S3). It has to be noted that in this way, only an apparent stability constant for one average Cd^{II} binding site within a MT is obtained. Hence all binding sites within a given MT are treated as equal and independent of each other. The values for all constructs used in this study are in the order of 10^{11} M^{-1}. The apparent binding constant to rabbit liver Cd_7MT2 was determined as a control and gave a log K_{app} value of 14.44 ± 0.07 in agreement with the literature (14.8) [33]. Hence the apparent stability constants of the investigated constructs are all lower than the one obtained for rabbit liver MT2, and are also lower than the ones of, for example, human MT-3 (14.3) [33] or nematode MT-1 and MT-2 (13.1 and 15.0, respectively) [49]. However, with a log K_{app} value of 11.94 ± 0.28 Cd_5cicMT2 has a higher binding constant than the bacterial MT from *Pseudomonas fluorescens* (log K_{Cd} 10.93) [32]. Lastly, the wheat E_c-1 protein from the plant MT subfamily 4 that features 17 Cys residues as ligands, has a log K_{Cd} value of roughly 12–13 [50], which is just slightly higher than the one of Cd_5cicMT2. This is consistent with the pH stability of both proteins. Also the pK_a value of Cd_5cicMT2 is by 0.1 units higher than the one of Cd_6E_c-1, equivalent with a slightly reduced overall pH stability of Cd_5cicMT2 compared to Cd_6E_c-1 [16,51]. Therefore, the results from the competition experiment with 5F-BAPTA are well in-line with results from the literature.

4. Conclusions

The results presented here provide the first comprehensive investigation of the metallation pathway of a plant MT2 protein. Investigating the folding of the full-length protein as well as of its separate domains in presence of certain metal ion concentrations is essential for understanding the role of MTs in the cellular environment. The stepwise metallation with Cd^{II} reveals formation of sub-metallated species, but no obvious positive cooperativity. This is advantageous in a

sense as it prevents high abundance of apo-MT species, which would be highly prone to proteolytic attack, while still offering ample free coordination sites to ensure efficient binding of any free metal ions (essential or toxic). In addition, non-coordinated Cys thiolate groups can act as reactive oxygen species scavengers. The metallation pathway presented here shows clearly that there is no preferential binding region (N- or C-terminal) for the first Cd^{II} ion, while additional equivalents, *i.e.* two and three, have a higher preference to coordinate to the N-terminal region. This might be, at least in part, facilitated by the larger number of Cys residues at the N-terminus (eight *versus* six). There is no obvious influence of the linker region on the binding capacity of individual domains. However, manipulation of the linker region, *e.g.* by introducing additional residues for TEV cleavage apparently affects early cluster formation (addition of less than 5 Cd^{II}). In the experiments with the N-TEV-C construct or with the 1:1 N1/C1 mixture, heterodimer Cd_5-cluster formation is only observed upon addition of 5 Cd^{II} ions. In contrast, a Cd5 cluster is already detected in the experiments with full-length cicMT2 or the 1:1 N2/C2 mixture after addition of 4 or 3 equivalents of Cd^{II}, respectively (Fig. 10). Hence while an intact linker seems to promote cluster formation, hetero-dimerization of the separate peptides is more efficient without additional residues from the linker region or even from a TEV cleavage site.

Abbreviations

MT	Metallothionein
cicMT2	*Cicer arietinum* (chickpea) MT
MALDI-MS	matrix-assisted laser desorption/ionization mass spectrometry
ESI-MS	electrospray ionization mass spectrometry
TEV	tobacco etch virus
DLS	dynamic light scattering
GST	glutathione S-transferase
LB	lysogeny broth
LB^{amp+}	lysogeny broth supplemented with ampicillin
PBS	phosphate buffered saline
EDTA	ethylenediaminetetraacetic acid
GSH	reduced glutathione
SEC	size-exclusion chromatography
TCEP	tris (2-carboxyethyl) phosphine hydrochloride
Tris	tris (hydroxymethyl) aminomethane
5F-BAPTA	1,2-bis- (2-amino-5-fluorophenoxy) ethane-*N*,*N*,*N*′,*N*′-tetra-acetic acid

Declaration of competing interest

The authors declare that they have no known competing financial interests or personal relationships that could have appeared to influence the work reported in this paper.

Acknowledgments

Financial support from the Swiss National Science Foundation (grant ID 200020_175623 to E.F.) and the “Biomolecular Structure and Mechanism PhD Program of the Life Science Zürich Graduate School” (A.S.) is gratefully acknowledged.

Appendix A. Supplementary data

Supplementary data to this article can be found online at https://doi.org/10.1016/j.jinorgbio.2020.111157.

References

[1] F.G. Gustafson, Plant Physiol. 21 (1946) 49–62.
[2] H. Wolters, G. Jürgens, Nat. Rev. Genet. 10 (2009) 305–317.
[3] J.-C. Amiard, C. Amiard-Triquet, S. Barka, J. Pellerin, P.S. Rainbow, Aquat. Toxicol. 76 (2006) 160–202.
[4] M. Brouwer, D.R. Winge, W.R. Gray, J. Inorg. Biochem. 35 (1989) 289–303.
[5] M.G. Cherian, Y.J. Kang, Exp. Biol. Med. 231 (2006) 138–144.
[6] C. Günes, R. Heuchel, O. Georgiev, K.H. Müller, P. Lichtlen, H. Blüthmann, S. Marino, A. Aguzzi, W. Schaffner, EMBO J. 17 (1998) 2846–2854.
[7] G. Roesijadi, Comp. Biochem. Physiol. C 113 (1996) 117–123.
[8] M. Vašák, D.W. Hasler, Curr. Opin. Chem. Biol. 4 (2000) 177–183.
[9] J.H.R. Kägi, S.R. Himmelhoch, P.D. Whanger, J.L. Bethune, B.L. Vallee, J. Biol. Chem. 249 (1974) 3537–3542.
[10] W. Feng, F.W. Benz, J. Cai, W.M. Pierce, Y.J. Kang, J. Biol. Chem. 281 (2006) 681–687.
[11] W. Maret, J. Nutr. 130 (2000) 1455S–1458S.
[12] F. Reinecke, O. Levanets, Y. Olivier, R. Louw, B. Semete, A. Grobler, J. Hidalgo, J. Smeitink, A. Olckers, F.H. Van der Westhuizen, Biochem. J. 395 (2006) 405–415.
[13] S. Suzuki, S. Tohma, N. Futakawa, M. Higashimoto, M. Takiguchi, M. Sato, J. Health Sci. 51 (2005) 533–537.
[14] J. Domènech, R. Orihuela, G. Mir, M. Molinas, S. Atrian, M. Capdevila, J. Biol. Inorg. Chem. 12 (2007) 867–882.
[15] O. Schicht, E. Freisinger, Inorg. Chim. Acta 362 (2009) 714–724.
[16] X. Wan, E. Freisinger, Metallomics 1 (2009) 489–500.
[17] J.N. Hegelund, M. Schiller, T. Kichey, T.H. Hansen, P. Pedas, S. Husted, J.K. Schjoerring, Plant Physiol. 159 (2012) 1125–1137.
[18] I.M. Armitage, T. Drakenberg, B. Reilly, Met. Ions Life Sci. 11 (2013) 117–144.
[19] X. Wan, E. Freisinger, Inorg. Chem. 52 (2013) 785–792.
[20] P.M. Gehrig, C.H. You, R. Dallinger, C. Gruber, M. Brouwer, J.H.R. Kägi, P.E. Hunziker, Protein Sci. 9 (2000) 395–402.
[21] M.E. Merrifield, Z.Y. Huang, P. Kille, M.J. Stillman, J. Inorg. Biochem. 88 (2002) 153–172.
[22] P. Palumaa, E. Eriste, O. Njunkova, L. Pokras, H. Jornvall, R. Sillard, Biochemistry 41 (2002) 6158–6163.
[23] K.E.R. Duncan, M.J. Stillman, FEBS J. 274 (2007) 2253–2261.
[24] D.E.K. Sutherland, M.J. Stillman, Biochem. Biophys. Res. Commun. 372 (2008) 840–844.
[25] G.W. Irvine, T.B.J. Pinter, M.J. Stillman, Metallomics 8 (2016) 71–81.
[26] T.T. Ngu, M.J. Stillman, J. Am. Chem. Soc. 128 (2006) 12473–12483.
[27] S.H. Chen, D.H. Russell, Biochemistry-Us 54 (2015) 6021–6028.
[28] S.H. Chen, W.K. Russell, D.H. Russell, Anal. Chem. 85 (2013) 3229–3237.
[29] R.B. Kapust, J. Tözser, J.D. Fox, D.E. Anderson, S. Cherry, T.D. Copeland, D.S. Waugh, Protein Eng. 14 (2001) 993–1000.
[30] T. Huber, E. Freisinger, Dalton Trans. 42 (2013) 8878–8889.
[31] J.E. Tropea, S. Cherry, D.S. Waugh, Methods Mol. Biol. 498 (2009) 297–307.
[32] J. Habjanic, O. Zerbe, E. Freisinger, Metallomics 10 (2018) 1415–1429.
[33] D.W. Hasler, L.T. Jensen, O. Zerbe, D.R. Winge, M. Vašák, Biochemistry 39 (2000) 14567–14575.
[34] O.I. Leszczyszyn, C.R.J. White, C.A. Blindauer, Mol. BioSyst. 6 (2010) 1592–1603.
[35] T.J.M. Schoenmakers, G.J. Visser, G. Flik, A.P.R. Theuvenet, Biotechniques 12 (1992) 870–878.
[36] R. Dallinger, Y.J. Wang, B. Berger, E.A. Mackay, J.H.R. Kägi, Eur. J. Biochem. 268 (2001) 4126–4133.
[37] G. Meloni, K. Zovo, J. Kazantseva, P. Palumaa, M. Vašák, J. Biol. Chem. 281 (2006) 14588–14595.
[38] H. Willner, M. Vašák, J.H.R. Kägi, Biochemistry 26 (1987) 6287–6292.
[39] A.C.S. Cabral, J. Jakovleska, A. Deb, J.E. Penner-Hahn, V.L. Pecoraro, E. Freisinger, J. Biol. Inorg. Chem. 23 (2018) 91–107.
[40] M. Berardini, T.J. Emge, J.G. Brennan, Inorg. Chem. 34 (1995) 5327–5334.
[41] T. Huber, (2013) PhD Thesis, University of Zurich, 2013.
[42] R.B. Kapust, J. Tözser, T.D. Copeland, D.S. Waugh, Biochem. Biophys. Res. Commun. 294 (2002) 949–955.
[43] J.A. Szymanska, A.J. Zelazowski, M.J. Stillman, Biochem. Bioph. Res. Co. 115 (1983) 167–173.
[44] S.H. Chen, L.X. Chen, D.H. Russell, J. Am. Chem. Soc. 136 (2014) 9499–9508.
[45] K.B. Nielson, C.L. Atkin, D.R. Winge, J. Biol. Chem. 260 (1985) 5342–5350.
[46] G. Singh, S. Tripathi, K. Shanker, A. Sharma, J. Biomol. Struct. Dyn. 37 (2019) 1520–1533.
[47] D.M. Smilgies, E. Folta-Stogniew, J. Appl. Chrystallogr. 48 (2015) 1604–1606.
[48] J. Benters, U. Flögel, T. Schäfer, D. Leibfritz, S. Hechtenberg, D. Beyersmann, Biochem. J. 322 (1997) 793–799.
[49] S. Zeitoun-Ghandour, J.M. Charnock, M.E. Hodson, O.I. Leszczyszyn, C.A. Blindauer, S.R. Stürzenbaum, FEBS J. 277 (2010) 2531–2542.
[50] O.I. Leszczyszyn, R. Schmid, C.A. Blindauer, Proteins Struct. Funct. Bioinform. 68 (2007) 922–935.
[51] J. Loebus, E.A. Peroza, N. Blüthgen, T. Fox, W. Meyer-Klaucke, O. Zerbe, E. Freisinger, J. Biol. Inorg. Chem. 16 (2011) 683–694.